Desalination and Water Treatment
www.deswater.com

doi:10.5004/dwt.2017.20367

68 (2017) 23–31
March

Temperature-dependent boron permeability through reverse-osmosis membranes: implications for full-scale simulations

Liron Ophek, Oded Nir*, Hadas Segal, Ori Lahav

Faculty of Civil and Environmental Engineering, Technion, Haifa 32000, Israel, email: odednir3@gmail.com

Received 2 June 2016; Accepted 9 October 2016

ABSTRACT

Boron removal from desalinated seawater is essential for obtaining high quality water, suitable for irrigation. Removal of boron by RO (reverse osmosis), the leading desalination technology, is significantly affected by variations in feed water temperature. Nevertheless, a widely agreed quantitative method for describing the temperature effect on the boric acid permeability constant, an important parameter in RO process modeling, was thus far unavailable. In this paper, different methods for describing permeability constants as a function of temperature were systematically evaluated against empirical results. It was demonstrated that non-specific temperature correlations, which are based on a single permeability measurement at a reference temperature, result in increased deviations from the measured permeability as the temperatures shift away from the reference value. A more accurate approach is to determine membrane-specific temperature correlations based on measured permeabilities at the relevant temperature range. Subsequently, the influence of accurate temperature correction on process modeling was assessed by comparing experimental boron rejections at practical conditions to simulation results. It was found that a reliable boric acid permeability coefficient is particularly significant at warm temperature, where boron rejection is less effective. Finally, implications to process design are discussed in light of accurate temperature dependent boron removal simulations.

Keywords: SWRO; Permeability constants; Boron; WATRO; Simulation

1. Introduction

Seawater desalination plants are required to address significant fluctuations in feed water temperature throughout the year. In some places, the temperature has been reported to change by up to 6°C during a given day [1] and on annual basis Mediterranean seawater temperature typically ranges from 14 to 31°C. It is well known that the quality of seawater reverse osmosis (SWRO) permeates changes as a function of temperature variations, affecting both the TDS and the boron concentration in the product water. In particular, the boron concentration in the permeate stream, which increases significantly as the temperature increases, poses a challenge to desalination plants, especially when the target concentration is low (e.g., 0.3–0.4 mg B/l, as required in recent bids in Israel and Spain). In places where strict limitations are enforced on both boron and TDS concentrations in the product water, a strong incentive exists to adjust SWRO operational conditions to account for temperature changes, since operational costs (particularly the specific energy consumption) may be significantly affected by changes in operational conditions. In a full-scale SWRO optimization study it was shown that a substantial cost difference existed between operation at constant conditions (conventional mode) and an optimal operation which takes into account adjustment to temperature changes [1].

At high temperatures, the trans-membrane water flux through RO membranes is increased; however, the diffusion rate of $B(OH)_3$ increases much more significantly, resulting in net reduction in the apparent $B(OH)_3$ rejec-

*Corresponding author.

tion [2,3]. In parallel, the apparent pK_a value of the boron weak acid system decreases at high temperature, resulting in higher overall concentration of the well rejected borate species ($B(OH)_4^-$ and complexes thereof) at a given pH value [4]. Moreover, the dissociation constants of water and other weak-acid systems (e.g., the carbonate system) are also affected by temperature, resulting in a change in pH which affects boron species distribution and thus its rejection. Furthermore, change in fluxes of other weak acid species (e.g., water and carbonate systems) due to temperature related changes in permeability or speciation may also indirectly affect boron permeability by inducing pH changes. Accounting for all these temperature effects in a simulation model for process design purposes requires a comprehensive modeling approach. In a previous work, we developed an advanced RO simulation program named WATRO (Weak Acids Transport in Reverse Osmosis) which accounts for acid-base dynamics, pH changes and their influence on weak acid species fluxes [5]. Although temperature effects on acid-base equilibrium are well accounted for in WATRO through the use of the PHREEQC software [6] thermochemical database, the effect on permeability constants was not evaluated experimentally in [5].

Several works have reported on mathematical terms correlating between the water temperature and the permeability values of boron, Na^+/Cl^- ("salt") and H_2O. Such data are essential for temperature-sensitive process design. Taniguchi et al. [7] developed a simulation model based on the Spiegler–Kedem and film-layer models which included adjustment of water and salt permeabilities according to both pressure and temperature. Temperature-related permeability correlations for NaCl and H_2O were determined from experimental data for two different membranes, and the model was verified by comparing simulated permeate flow and permeate ion concentrations to empirical data from an actual RO plant. Deviations up to 15% were observed between calculated and experimental results, recorded mainly at the high temperature operation conditions. Boron rejection was not considered in this study. Working with four different (flat sheet) SWRO membranes Hyung and Kim [2] fitted exponential temperature correlations to the permeabilities of boric acid and borate ion, based on the Kedem–Katchalsky transport model coupled with the film-layer theory. Surprisingly, temperature effect was highly similar for all four membranes and was conveniently represented by a single exponential function. In contrast, in a different study [3] two separate set of parameters were required in order to correlate boric-acid permeability for the two SWRO membranes used. The temperature correlation used in this study was of Arrhenius type, while the RO transport model was solution-diffusion. The predicted boron concentration at varying temperatures reasonably matched the experimental results obtained at low recovery using a bench-scale RO system. In their theoretical work on boron removal from SWRO, Sassi and Mujtada [8] developed a nonlinear minimization optimization based on the solution diffusion and film-layer transport models, whereas P_S, P_W and P_B were adjusted to temperature by normalizing the dynamic viscosity of the water at the target temperature relative to a reference temperature. This approach (referred here as the "Stokes-Einstein relation") which is based on the Stokes–Einstein diffusivity equation is considered to be general, since it does not encompass membrane specific parameters.

Considering the above mentioned studies, it can be concluded that a widely accepted approach for relating permeability coefficients to temperature, especially in the case of boric acid, is currently missing from the scientific literature. Furthermore, experimental evaluation of temperature dependent model predictions for boron transport has not been conducted at practical SWRO conditions, that is, high recovery ratio (40–50%) and spiral wound modules. Therefore, this work is focused on systematic evaluation and comparison of different temperature-based correlations for permeability terms using a typical spiral wound SWRO element. First, correlations were assessed by comparing them with empirical permeability constants determined from low recovery experiments. Then, the correlations were embedded in a full-scale SWRO model and the predicted rejections were compared with high recovery experimental results. Through these steps, we provide a quantitative assessment for the magnitude of errors and uncertainties in model predictions stemming from the use of general temperature-permeability correlations and address the questions of under which conditions specific temperature calibration for each membrane is required and whether or not a significant improvement in model predictions can be obtained by this practice. Finally, using the most accurate temperature dependence terms, we project the effect of temperature on SWRO boron removal and discuss implications for energy consumption and water productivity.

2. Materials and methods

2.1. Determination of permeability constants

SWRO experiments were performed using a pilot-scale RO system described in detail in [9]. In all calibration experiments, the operating pressure ranged from 38 to 62 bars. The pressure was typically increased during a given experiment to result in 8–9 different pressure points, while the feed flow-rate was independently adjusted using a frequency converter and maintained constant. The (fully re-circulated) system was allowed to stabilize for ~15 min each time before sampling. Temperature, conductivity, pressure and flow rates were continuously recorded by digital meters connected to a computer and in all calculations averaged values (over 2–3 min) of the recorded parameters were used. The system includes a titanium plate heat exchanger (ORZ2 of "Oran", capacity: 15154.2 kcal/h) and a chiller (CWA-36TPS, capacity: 9,000 Kcal/h) for maintaining constant temperatures of 14, 20, 25 and 31 ± 0.5°C (three repetitions were performed at each temperature). A 4" Hydranautics commercial membrane (SWC5-4040) was used, which was characterized by the following data (obtained from the manufacturer at standard conditions): salt rejection 99.7%; active surface area 7.9 m^2 and permeate flow rate 7.2 m^3/d (data for standard boron rejection was not supplied). The membrane was conditioned before use by circulating seawater at 65 bar for 1 h. Filtered Mediterranean seawater was collected from Ma'agan Michael

(Israel). Seawater pH was adjusted to pH 6.0–6.5 using HCl. At this pH range, boric-acid practically constitutes the whole concentration of the boron weak-acid system. Samples for analyses were taken from the feed, brine and permeate stream at the varying trans-membrane pressure points. For comparison purposes, another three similar calibration experiments were performed with a 4″ Hydranautics high-flux membrane (SWC6-4040), characterized at standard conditions as follows (manufacturer data): salt rejection 99.7%; B rejection 91%; active surface area 7.9 m^2 and permeate flow rate 9.46 m^3/d.

The results obtained from the calibration experiments were used to calculate boron and salt permeability constants according to the Solution Diffusion model ($P_{B(OH)3}$, k_{BOH3}, P_S, k_S) using two computation techniques: Non-linear optimal curve fitting and the Osmotic Pressure Method [10]. To yield the error-minimization term, the solute transport (Eq. (1)) was combined with the film-layer model (Eq. (2)) to yield Eq. (3):

$$J_s = J_v C_p = P_s\left(C_m - C_p\right) \tag{1}$$

$$\frac{J_v}{k} = \ln\left[\left(C_m - C_p\right)/\left(C_b - C_p\right)\right] \tag{2}$$

$$\frac{C_b - C_p}{C_p} = \frac{J_v}{P_{B(OH)_3} e^{J_v/k}} \tag{3}$$

Eq. (4) represents the non-linear curve-fitting optimization equation.

$$Minimize\left\{\sum_{i=1}^{n}\left(\frac{C_{bi} - C_{pi}}{C_{pi}} = \frac{J_{vi}}{P_{B(OH)_3} e^{J_{vi}/k}}\right)^2\right\} \tag{4}$$

The optimization problem was solved by MATLAB using the specific solver "fminsearch", which is based on the Nedler-Mead Simplex algorithm. Both the $B(OH)_3$ permeability and the mass transfer coefficient were calculated using ~1,000 different initial guesses for each results set. The two constants were calculated three times for each temperature.

The Osmotic Pressure method (for details, refer to Section 2 and 3 in the SM file) is considered more robust in case of high TDS rejections, due to the large difference between C_b and C_p, which can amount to 2–3 orders of magnitude. Since large variation in the concentration values may yield a considerable error when the Optimization Method is used we chose to apply the Osmotic Pressure Method to extract P_S and k_S (e.g., applying the Optimization Method for salts showed a significant difference of 3–4 orders of magnitude in the objective function value, as compared with boron).

To execute the Osmotic Pressure Method, the water transport equation (Eq. (5)) was first rewritten in an expanded form (Eq. (6)):

$$J_v = P_w\left(\Delta P - \Delta\pi\right) \tag{5}$$

$$J_v = P_w\left(\Delta P - \left(\phi_m C_m RT - \phi_p C_p RT\right)\right) \tag{6}$$

Then, using the measured results, the concentration near the membrane wall (C_m) was calculated using Eq. (7):

$$C_m = \frac{1}{\phi_m}\left\{\phi_p C_p - \frac{1}{RT}\left(\frac{J_v}{P_w} - \Delta P\right)\right\} \tag{7}$$

Where ϕ is the osmotic coefficient, calculated for each specific average feed and concentrate composition using the Pitzer model embedded in PHREEQC.

Once C_m was known, k_S was determined using Eq. (2) from the slope of the plot of J_v vs. $ln[(C_m - C_p)/(C_b - C_p)]$ and P_S was determined using Eq. (1) from the slope of the plot of J_v vs. $(C_m - C_p)/C_p$. The permeability for water was determined experimentally using deionized water, according to Eq. (5) (J_v vs. ΔP).

After this procedure had been implemented to obtain all the required constants at each temperature, all the permeability values were fitted a temperature-dependence term valid for the tested temperature range. The temperature-dependence terms were then embedded in the WATRO simulation code [5] in order to validate the correlations obtained in the work and compare them with previously published terms.

2.2. Empirical versus simulated rejections at high recovery

High recovery experiments were performed using the same pilot scale system described above at a constant pressure of 66 ± 0.5 bars. The recovery ratio was increased by collecting permeate to a different tank until a recovery ratio of 47% ± 2% was attained. For each sampled recovery ratio, the system was operated in a full recirculation mode for ~15 min before sampling. Nine experiments (three temperature values, three repetitions per temperature) were performed; during each five samples were taken, representing recovery ratios equal or lower than 47%. The samples were taken from the (cumulative) stirred permeate tank, the momentarily produced permeate, the feed stream and the momentarily produced brine stream. The experimental results were compared with simulated results obtained by the WATRO program. In the runs performed here, WATRO was embedded with the terms developed in this work.

2.3. Analyses

All samples taken from the feed, brine, permeate, and accumulated permeate streams at each experimental point were analyzed for boron and major ion concentrations by ICP-AES (1CAP6300 Duo, Thermo Scientific). The pH value of the feed water at the beginning and at the end of the experiment was measured with a Metrohm Aquatrode Plus (6.0257.600) combined glass electrode with integrated Pt 1000 temperature sensor and a Metrohm780 pH meter calibrated by NIST buffers with the addition of 0.75 M NaCl, according to the procedure described in [11]. The aim was to achieve consistency with the WATRO program which is coupled with the PHREEQC software [6] so that the pH calculations would conform to the Pitzer ion-interaction approach.

3. Results and discussion

As a first step, the permeability coefficients of H_2O and TDS through the SWC5-4040 SWRO element were obtained at four temperature values. As seen in Fig. 1, the permeabilities for water were determined from pure water flux experiments, while TDS permeabilities were obtained from flux and rejection results using real seawater as feed. Concentration polarization was accounted for by determining the concentration near the membrane using the osmotic-pressure method (see Eq. (5) in Section 2). This method was found superior in terms of fitting filtration results compared with the alternative which is based on non-linear optimization of the solution-diffusion-film transport model (Eqs. (3)–(4) in Section 2). In both cases, temperature dependency was well described by an exponential term. The Stokes–Einstein relation produced a similar trend, however, with larger deviations from the measured permeabilities at low and high temperatures (results not shown), highlighting the need for membrane-specific temperature calibration if accurate projections are desired. Evidently, water flux at increased recovery ratios was more accurately predicted by the simulation program embedded with the membrane-specific correlations compared with the general Stokes–Einstein relation. For example, the apparent water flux at 47% recovery (31°C; 66 bar) was $2.1{\cdot}10^{-6}$ [$m^3/m^2{\cdot}s$], while membrane-specific correlations predicted $1.98{\cdot}10^{-6}$ [$m^3/m^2{\cdot}s$] and general Stokes–Einstein correlations prediction was $1.83{\cdot}10^{-6}$. TDS rejections were more accurately predicted by the simulation program embedded with the membrane-specific correlations as well (see Fig. 1(a)–(c). in the Supplementary Material). It should be noted that the apparently accurate correlation of salt permeability obtained by the Stockes-Einstein is questionable, since errors in the water permeability for the same correlation propagate to the calculated salt permeability values. Accurate simulation of the water flux is imperative for accurate prediction of boron permeate concentrations due to the significant effect that the water flux has on the apparent rejection of solutes.

The empirical $B(OH)_3$ permeability temperature dependency was best described by a linear term (R^2 = 0.998) as shown in Fig. 2. This is somewhat surprising since previous general correlations were fitted by an exponential trend [2, 3], this might have emerged whether permeability has been measured at a wider temperature range. However, the linear correlation shown here covers the entire temperature range of the Mediterranean Sea coastal water and is therefore practical in the context of Mediterranean SWRO desalination. Also shown in Fig. 2 are the Stock–Einstein diffusion relation and the exponential correlation found appropriate by Hyung and Kim [2] for four different membranes; both terms can be applied for calculating permeability at a given temperature based on an empirical permeability at a reference temperature. These non-specific relations increasingly deviated from the experimental permeabilities as temperatures shifted away from the reference temperature (25°C). As a result, at 14°C the largest difference between the permeabilities predicted by each method was observed. This emphasizes the bias affected by the choice of reference temperature in case a single permeability value is used along with a non-specific correlation. In contrast, specific correlation requires additional experiments (typically 3–4); however, the error is unaffected by the distance from an arbitrary reference temperature and is therefore smaller.

As seen in Fig. 2, the permeabilities predicted by the Stokes–Einstein relation were closer to the measured values, compared with the Hyung and Kim correlation, especially at the lower temperature range. However, while this was true for the SWC5 membrane element, permeability values measured for a different membrane, SWC6-4040, resulted in a different conclusion. In contrast with the linear term obtained with SWC5-4040 (a common-flux membrane) the best correlation of $B(OH)_3$ permeability with temperature (depicted in Fig. 3) obtained with the high-flux SWC6-4040 membrane was exponential. In this case, the measured permeabilities were better described by the Hyung and Kim correlation, while the Stocks–Einstein relation yielded relatively large deviations (Fig. 3). Despite being produced by the same manufacturer, these two SWRO membrane elements responded differently to changes in temperature, a finding which further emphasizes the benefits of temperature-dependent characterization as opposed to relying on a single permeability constant and non-specific temperature correction terms.

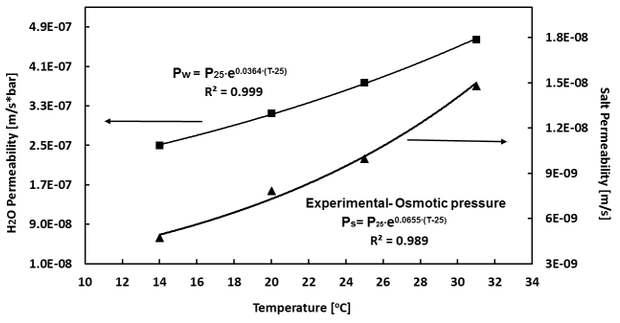

Fig. 1. Permeability of water (P_W) and salts (P_S) as a function of temperature. Squares represent water permeability experimental results (n = 1). Note: Triangles represent salt permeability experimental results (n = 3), determined using the osmotic pressure method, both obtained with SWC5-4040.

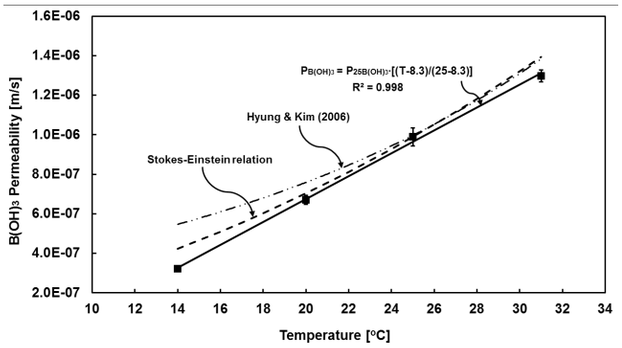

Fig. 2. Permeability of boric acid ($P_{B(OH)3}$) as a function of temperature. Squares represent experimental results obtained with SWC5-4040 (n = 3). The full line represents linear curve fitting of the empirical results. Dashed lines represent Hyung and Kim's [2] exponential correlation and the Stokes–Einstein relation.

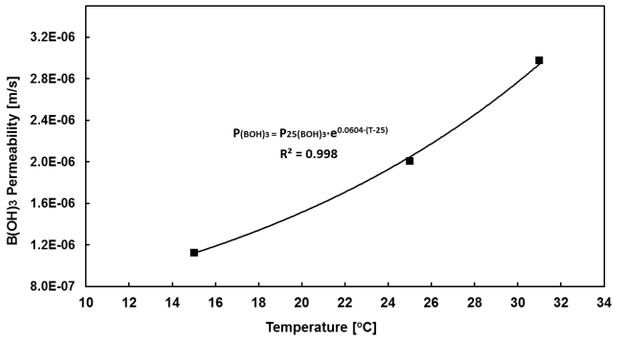

Fig. 3. Permeability of boric acid ($P_{B(OH)3}$) as a function of temperature. Squares represent experimental results obtained with SWC6-4040 (n = 1). The full line represents exponential curve fitting of the empirical results.

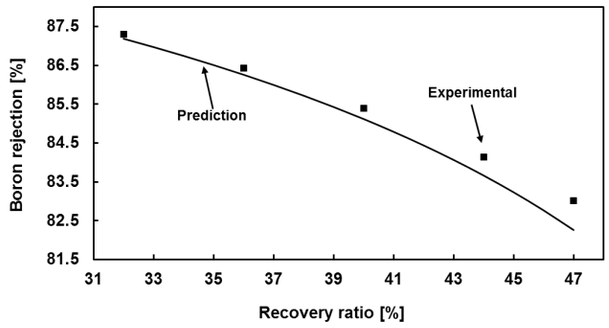

Fig. 4. Boron predictions by the WATRO program embedded with current-work correlations (Model 1 – full line) and the experimental results (squares) at different recovery ratios (24°C; SWC5-4040 membrane; n = 3).

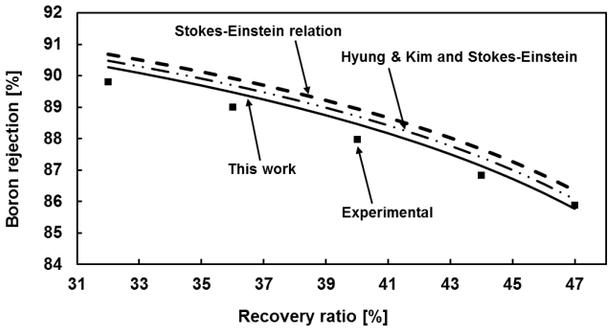

Fig. 5. Boron rejection predictions by the WATRO program embedded with current-work correlations (Model 1 – full line), previous literature correlations (Models 2 and 3 – dashed lines) and the experimental results (squares) at different recovery ratios (18°C; SWC5-4040 membrane; n = 3).

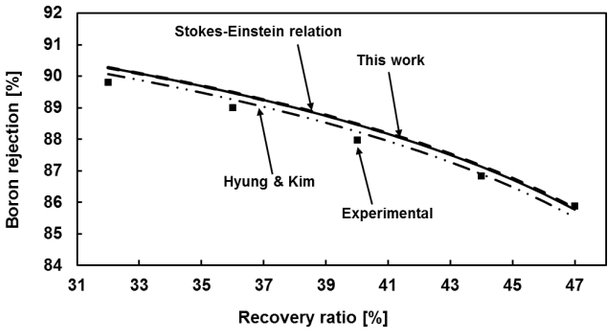

Fig. 6. Boron rejection predictions by the WATRO program embedded with current-work correlations (Model 1 – full line), current P_w and P_S correlations combined with previous literature $P_{B(OH)3}$ correlations (Models 4 and 5 – dashed lines) and the experimental results (squares) at different recovery ratios (18°C; SWC5-4040 membrane; n = 3).

The permeability terms shown above indicate that the largest deviations of simulated permeate quality from measured results can be expected to occur at the extreme temperatures on both sides of the range. In order to evaluate the process design implications of membrane-specific vs. non-specific temperature corrections, practical recovery ratio (47%) SWRO experiments were performed at 18°C and 31°C and the obtained empirical results were compared with WATRO simulation results attained using different combinations of permeability constants. The following combinations were embedded in the WATRO simulation program: (1) The membrane-specific correlations obtained in this work for H_2O, TDS and boric acid; (2) Stokes–Einstein correlations for H_2O and TDS, combined with the Hyung and Kim correlation [2] for boric acid; (3) Stokes–Einstein correlation for H_2O, TDS and boric acid (4) The membrane-specific correlations obtained in this work for H_2O combined with the Hyung and Kim correlation for boric acid; (5) The membrane-specific correlations obtained in this work for H_2O, TDS combined with the Stokes-Einstein relation for boric acid.

A preliminary estimation of the model accuracy was obtained by performing a validation experiment (47% recovery ratio) at the reference temperature, 24°C, wherein the different correlations converge (see Fig. 2). As shown in Fig. 4 the rejection of boron was accurately predicted by the simulation at the practical recovery ratios. As expected, model errors increased with recovery ratio, however the maximum deviation in rejection was ~1%, which translates to a deviation of ~0.03 mg B/l in the B permeate concentration, that is, well within reasonable measurement error. Therefore, larger deviations appearing at colder and warmer conditions can be safely attributed to temperature effects.

Figs. 5 and 6 show the results obtained from the experiments vs. the simulation runs at 18°C. When sets of constants (i.e., non-specific permeabilities for H_2O, TDS and boric-acid vs. specific correlations obtained in this work as shown in Fig. 5) were compared, boron rejections were best predicted by the simulations in which the temperature correlations for the specific membrane produced in this work were used. When the tested models differed only in terms of boron temperature correlations (boric-acid permeability parameter was isolated), the difference in predicted boron rejection was much smaller (as seen in Fig. 6), indicating that the accuracy of boron rejection simulation was more influenced by the water flux projections than by the boric-

acid permeability at this temperature. This observation may be related to the low permeability of boric-acid at low temperature. It is noted that not only permeability correlations were updated in the WATRO program due to the calibration experiments: the temperature dependency of the mass transfer coefficient was also adjusted specifically for the empirically tested temperatures.

In general, the variations in the predicted boron rejection, as well as the deviations from experimental results obtained by the different combination of model parameters were very small and almost insignificant at 18°C. However, this was not the case at 31°C, which represents the peak of summer in Mediterranean coastal water. As seen in Figs. 7 and 8, a very accurate prediction was observed towards boron rejection by the WATRO program embedded with the membrane specific correlations at 31°C, whereas the use of non-specific temperature correlations resulted in significant deviations from experimental boron rejections. Similarly to 18°C, the combined effect of non-specific temperature-corrected permeabilities was indicated by the decreased deviations recorded when only specific correlations were used for water and TDS, as shown in Fig. 8. However, at 31°C, the differences were significant also in this case, demonstrating yet again that specific calibration for boron permeability is needed for obtaining an accurate prediction.

A comparison of five combinations of permeability coefficients discussed in this work is shown in Fig. 9. Empirical results obtained for boron permeate concentrations at 47% recovery are depicted along with the predictions of the five simulation data sets evaluated in this work. While at 18°C the deviation of all the models from the experimental results was small, it can be seen that at 31°C, which is the most critical temperature for process design purposes (since boron flux through the membrane is the highest), a large deviation of above 20% may be encountered when the simulation program does not include membrane-specific permeability terms adjusted for temperature (at 24°C the results were almost identical as discussed above). It can be seen in Fig. 9 that using the Stokes–Einstein relation for adjusting all permeabilities (Model 3) resulted in relatively small deviation (~10% or 0.08 mgB/l) for this specific membrane; however, this conclusion may not hold true for different membranes, as mentioned above. Thus, for being on the safe side, obtaining specific empirical correlations for the employed membrane is strongly recommended.

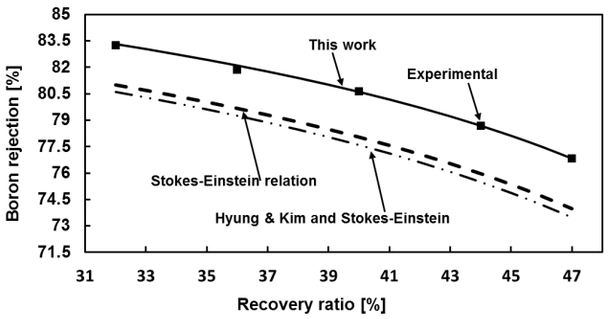

Fig. 7. Boron predictions by the WATRO program embedded with current-work correlations (full line), previous literature correlations (dashed lines) and the experimental results (squares) at different recovery ratios (31°C; SWC5-4040 membrane; $n = 3$).

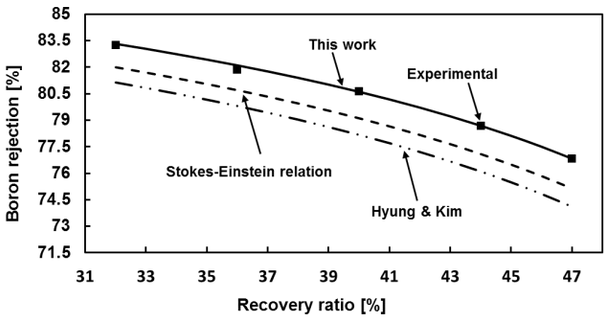

Fig. 8. Boron predictions by the WATRO program embedded with current-work correlations (full line), current P_w and P_S correlations combined with previous literature $P_{B(OH)3}$ correlations (dashed lines) and the experimental results (squares) at different recovery ratios (31°C; SWC5-4040 membrane; $n = 3$).

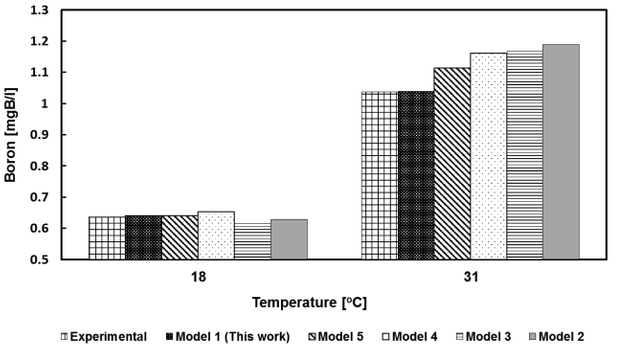

Fig. 9. Boron concentrations at 47% recovery: experimental results vs. WATRO simulations (current work correlations) and previous literature correlations.

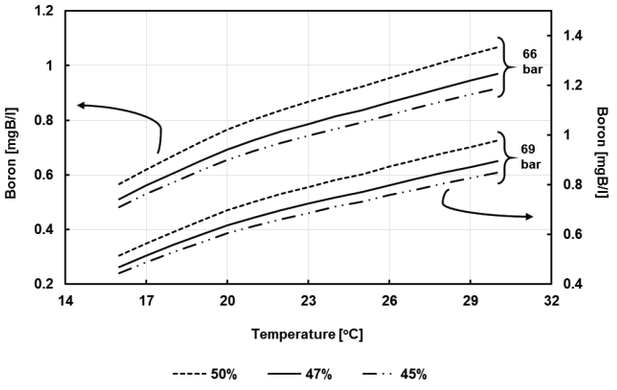

Fig. 10. Boron permeate concentrations projected by the WATRO program embedded with current-work membrane-specific correlations at different recoveries (45%, 47% and 50%) and operational pressures (66 and 69 bar) as a function of temperature (typical range for Mediterranean seawater). Feed pH and boron concentration were 8.2 and 5 mg/l, respectively.

The membrane-specific correlations obtained in this work for boric acid, water and TDS were embedded in the SWRO simulation program (WATRO) to produce accurate projections of boron permeate concentrations as a function of temperature at different operational conditions. The simulation results shown in Fig. 10 reveals the prospect of temperature sensitive optimization of energy consumption and water productivity by adjusting the pressure and recovery ratio, while keeping boron permeate concentrations regulated. For example, if the required boron concentration is 1 mg/l (e.g., California and EU drinking water standards), it may be beneficial to apply lower pressure in winter in order to save energy, while gradually increasing it as seawater temperature increase. The simulation results also indicate that the strictest boron regulations of 0.3–0.4 mg/l (e.g., Israel) cannot be met by a single SWRO pass (at ambient seawater pH). In this case, temperature-sensitive design and optimization should be performed simultaneously for the SWRO step and a post treatment step aimed specifically at boron removal (i.e., 2nd RO pass or ion exchange). Alternatively, to avoid the post-treatment step, the pH of the seawater feed could be altered as suggested in [9]. Incorporating appropriate temperature permeability correlations (as the ones obtained in this work) in the WATRO code enables both pH and temperature to be accurately considered in the simulation, thus potentially improving SWRO process design. Temperature and pH sensitive design in a two-pass system with strict boron requirements will be addressed in a future work.

Symbols

C_b	—	Solute concentration in the feed side bulk, [mol/l]
C_m	—	Solute concentration near the membrane, [mol/l]
C_p	—	Permeate solute concentration, [mol/l]
J_s	—	Solute flux, [mol/s]
J_v	—	Permeate flux, [m/s]
k	—	Mass transfer coefficient, [m/s]
P_{BOH3}	—	Boric acid permeability coefficient, [m/s]
P_s	—	Salt permeability coefficient, [m/s]
P_w	—	Water permeability coefficient, [m/s/bar]
ΔP	—	Trans-membrane pressure, [bar]
$\Delta\pi$	—	Trans-membrane osmotic pressure, [bar]
Φ	—	Osmotic coefficient, [–]

Acknowledgement

This project was funded by the Israel Science Foundation (#163/14).

References

[1] A. Jiang, J. Wang, L.T. Biegler, W. Cheng, C. Xing, Z. Jiang, Operational cost optimization of a full-scale SWRO system under multi-parameter variable conditions, Desalination, 355 (2015) 124–140.

[2] H. Hyung, J.H. Kim, A mechanistic study on boron rejection by sea water reverse osmosis membranes, J. Membr. Sci., 286 (2006) 269–278.

[3] P.V.X. Hung, S.H. Cho, S.H. Moon, Prediction of boron transport through seawater reverse osmosis membranes using solution–diffusion model, Desalination, 247 (2009) 33–44.

[4] O. Nir, O. Lahav, Chapter 14 – Single SWRO pass boron removal at high pH: prospects and challenges, In Boron Separation Processes, N. Kabay, M. Bryjak, N. Hilal, eds., Elsevier, Amsterdam, 2015, pp. 297–323.

[5] O. Nir, L. Ophek, O. Lahav, Acid–base dynamics in seawater reverse osmosis: experimental evaluation of a reactive transport algorithm, Environ. Sci.: Water Res. Technol., 2 (2016) 107–116.

[6] D.L. Parkhurst, C. Appelo, User's guide to PHREEQC (Version 2): a computer program for speciation, batch-reaction, one-dimensional transport, and inverse geochemical calculations, United States Geological Survey, USA (1999).

[7] M. Taniguchi, M. Kurihara, S. Kimura, Behavior of a reverse osmosis plant adopting a brine conversion two-stage process and its computer simulation, J. Membr. Sci., 183 (2001) 249–257.

[8] K.M. Sassi, I.M. Mujtaba, MINLP based superstructure optimization for boron removal during desalination by reverse osmosis, J. Membr. Sci., 440 (2013) 29–39.

[9] L. Ophek, L. Birnhack, O. Nir, E. Binshtein, O. Lahav, Reducing the specific energy consumption of 1st-pass SWRO by application of high-flux membranes fed with high-pH, decarbonated seawater, Water Res., 85 (2015) 185–192.

[10] M. Taniguchi, S. Kimura, Estimation of transport parameters of RO membranes for seawater desalination, AIChE J., 46 (2000) 1967–1973.

[11] O. Nir, E. Marvin, O. Lahav, Accurate and self-consistent procedure for determining pH in seawater desalination brines and its manifestation in reverse osmosis modelling, Water Res., 64 (2014) 187–195.

Supplementary Material

The effect of seawater temperature on boron removal by reverse osmosis

LironOphek, Oded Nir*, Hadas Segal, Ori Lahav

Faculty of Civil and Environmental Engineering, Technion, Haifa, Israel, 32000, email: odednir@campus.technion.ac.il

Content:

1. TDS prediction by WATRO embedded with different correlations compared with experimental results at different temperatures and recoveries

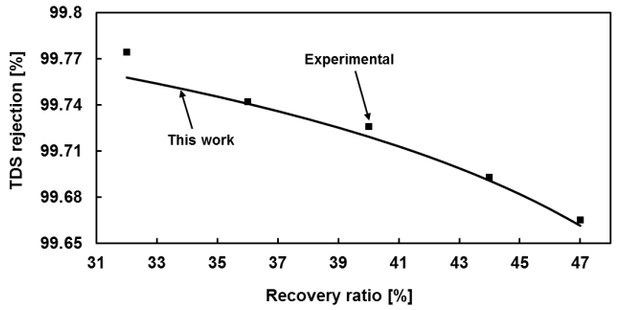

Fig. 1(a). TDS predictions by WATRO program embedded with current-work correlations (Model1 – full line) and the experimental results (squares) at different recovery ratios (24°C; SWC5-4040 membrane; n = 3).

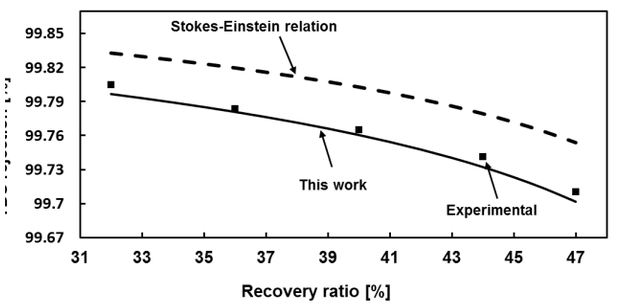

Fig. 1(b). TDS predictions by WATRO program embedded with current-work correlations (Model. 1 – full line), previous literature correlations (Model 3 – dashed lines) and the experimental results (squares) at different recovery ratios (18°C; SWC5-4040 membrane; n = 3).

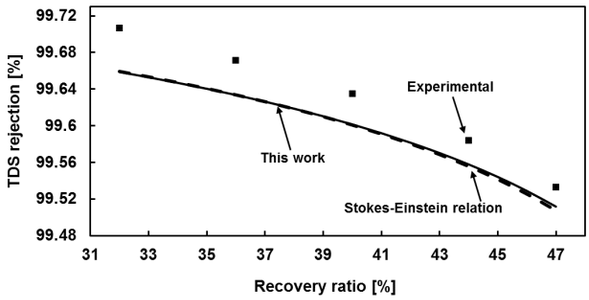

Fig. 1(c). TDS predictions by WATRO program embedded with current-work correlations (Model 1 – full line), previous literature correlation (Model 3 – dashed line) and the experimental results (squares) at different recovery ratios (31°C; SWC5-4040 membrane; n = 3).

2. Application of the osmotic pressure method for extraction of P_s and k_s

In order to extract P_s and k_s, samples from the feed and brine streams were taken at different operating pressure points, major ions concentrations were averaged and summed up to yield "Ctotavg", which represents the total concentration of salts in the brine (C_b).

Bt avg [M]	[Ca2+] avg [M]	[K+] avg [M]	[Mg2+] avg [M]	[Na+] avg [M]	[SO4-2] avg [M]	[Cl-] avg [M]	Ctot avg [M]
0.0004467	0.01206	0.0142	0.05831	0.57612	0.03677	0.6575255	1.35544
0.0004533	0.01214	0.01466	0.05806	0.57323	0.03672	0.6548496	1.3501
0.0004552	0.01211	0.01429	0.05857	0.57705	0.03684	0.6590295	1.35834
0.000448	0.01216	0.01448	0.05861	0.58041	0.03675	0.6629236	1.36578
0.0004496	0.01219	0.01445	0.05862	0.58087	0.03687	0.6631969	1.36665
0.0004615	0.01225	0.01446	0.05892	0.5835	0.0371	0.6660986	1.3728
0.000465	0.01232	0.01451	0.05917	0.58546	0.03731	0.6683218	1.37755
0.0004589	0.01245	0.01494	0.06005	0.59042	0.03747	0.6754164	1.39121
0.0004588	0.01248	0.01484	0.05974	0.59259	0.03755	0.6767646	1.39442

Fig. 2(a). Averaged concentration of major ions in the feed and brine streams.

Jv [m^3/m^2*sec]	P [bar]	T C°	Pw [m/sec*bar]	Cp [M]	øm	øp	Cm [M]	Lan(Cm-Cp/Cb-Cp)	(Cm-Cp)/Cp
1.58861E-06	38.43	13.94	2.49782E-07	0.004970175	0.9028	0.98192	1.49327	0.097181451	299.4457842
2.11392E-06	41.52	14.19		0.003879958	0.90263	0.98385	1.53817	0.130761752	395.4390331
2.55907E-06	44.51	13.92		0.003153426	0.90285	0.9853	1.59304	0.15972165	504.1774842
3.02743E-06	47.46	13.81		0.00271324	0.9031	0.98601	1.64198	0.184508025	604.1713966
3.4789E-06	50.21	13.96		0.002398627	0.90306	0.98635	1.68542	0.209983267	701.6604527
4.02532E-06	53.72	14.13		0.002072801	0.90313	0.98776	1.74627	0.240951154	841.4678612
4.40928E-06	56.33	14.31		0.001871829	0.90316	0.9883	1.79574	0.265429612	958.3516882

Fig. 2(b). Example of all the required data for calculating C_m according to Eq. (7).

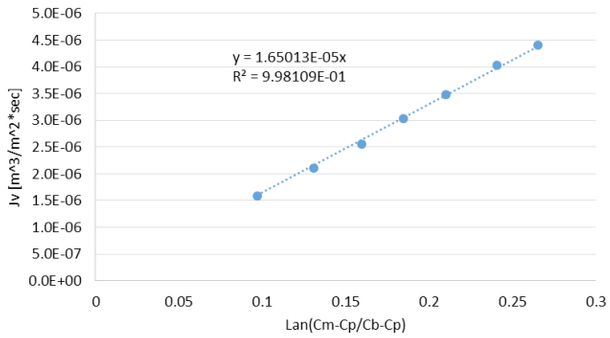

Fig. 2(c). Example of J_v vs. $\ln[(C_m - C_p)/(C_b - C_p)]$, the slope represent k_S according to Eq. (2).

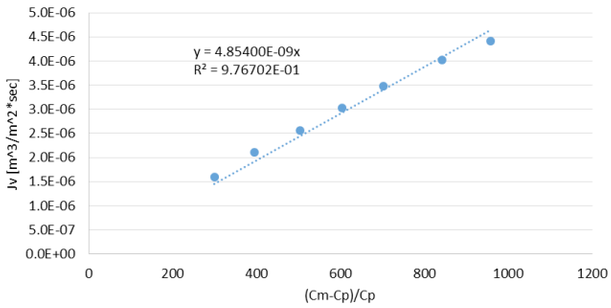

Fig. 2(d). Example of J_v vs. J_v vs. $(C_m - C_p)/C_p$, the slope represent P_S according to Eq. (1).

According to Eq. (2), the knowledge of C_p, C_m and J_v is also necessary. C_p was taken directly from permeate samples analyses, J_v was measured volumetrically during the experiment and C_m was calculated according to Eq. (7).

For the evaluation of C_m, f_m and f_p were calculated with PHREEQC (pitzer database): f_m according to the major ions content listed in Fig. A1 and f_p according to the analyzed concentration of the permeate stream.

P_w was extracted from a simple experiment executed with diluted water ($\Delta\pi = 0$) according to Eq. (5). According to Eq. (2) and (1) plot of J_v vs. $\ln[(C_m - C_p)/(C_b - C_p)]$ and J_v vs. $(C_m - C_p)/C_p$ was used to produce k_S and P_S, respectively.

3. Matlab code for the optimization method for extraction of $P_{B(OH)3}$ and $k_{B(OH)3}$.

The following MATLAB code can be used for implementing the Optimization Method:

```
% This function finds the SSE (Eq. (4)) of 8 experimental points set: Jv, Cp and Cb (the number of points can differ from 8; just update the 'for' loop to the suitable number).
% Update the vectors: Jv, Cp and Cb in the code function according to your data
% The input for "fminsearch" (minimization function) is an initial guess for the constants.
% For example: x0=[0.00000001;0.0003] while the first value is the permeability and the second is the mass transfer coefficient
%%%% Finally, run the minimization function:fminsearch(@findconst,x0)
function Mistake= findconst (x)
P=x(1);
k= x(2);
% Results
Jv=[2.0865E-06
2.60338E-06
2.98101E-06
3.99578E-06
4.44726E-06
4.89662E-06
5.24262E-06
5.76793E-06
];
Cp=[0.000117307
9.7513E-05
8.63349E-05
7.03053E-05
6.54848E-05
6.17277E-05
5.71478E-05
5.29638E-05
];
Cb=[0.000469128
0.000467905
0.000467562
0.000473825
0.000480723
0.000486471
0.000493223
0.000499485
];
mistake=zeros(1,8);
fori=1:8
mistake(i)=(((Jv(i)/(P*exp(Jv(i)/k))) – ((Cb(i)-Cp(i))/Cp(i)))^2); %Eq. (4)
end
Mistake=sum(mistake);
```